Inorg. Chem. **1993,** *32,* 101-105 **101**

New Strontium Borate Halides: $Sr_5(BO_3)_3X$ (X = F, Br)

Theodore Alekel III and Douglas A. Keszler*

Department of Chemistry and Center for Advanced Materials Research, Gilbert Hall 153, Oregon State University, Corvallis, Oregon 97331-4003

Received July 29, 1992

Two new strontium borate halides, $Sr_5(BO_3)_3F$ and $Sr_5(BO_3)_3Br$, have been synthesized and structurally characterized by single-crystal X-ray diffraction techniques. The two compounds are structurally similar, 3-dimensional frameworks of interconnecting Sr polyhedra and orthoborate groups but do not crystallize with the same symmetry. The fluoride forms in the centrosymmetric orthorhombic space group, *Pnma*, with cell parameters $a = 7.220$ (2) Å, $b = 14.092$ (2) Å, $c = 9.810$ (1) Å, and $Z = 4$. Three distinct Sr-centered O environments exist in this structure: distorted SrO_7F undecahedra, irregular SrO_6F coordination sites, and distorted SrO_8 square antiprisms, monocapped by a very weak Sr–O interaction of 3.04 Å. A trio of Sr atoms caps each F atom to form a shallow pyramid. $Sr_5(BO_3)_3Br$ crystals are also orthorhombic in the noncentrosymmetric space group $C222_1$ with $a = 10.002$ (2) Å, $b = 14.197$ (1) Å, $c = 7.458$ (2) Å, and $Z = 4$. Four Sr-centered polyhedra join to each other: distorted SrO_7Br_2 tricapped trigonal prisms, irregular octacoordinate SrO_6Br_2 undecahedra, and two dissimilar SrO_8 distorted square antiprisms. Six Sr nearest neighbors bond to each Br atom and define Sr octahedra that share triangular faces along the *c* direction to form zigzag chains.

Introduction

For many years haloapatites $[(Ca,Sr)_5(PO_4)_3(Cl,F)]$ have been employed as host materials in commercial phosphors for fluorescent lighting.[1] Their robust physical properties coupled with high quantum efficiencies have made them standard phosphor hosts for optically active dopants such as Sb^{3+}, Mn^{2+}, and Eu^{2+}.[2]

Borates also intrinsically possess characteristics that are advantageous for optical materials, which include high photon flux damage thresholds and wide optical transparency windows.[3] The commercial material $(Ce,Gd)MgB_5O_{10}$:Tb^{3+}, which converts 254-nm Hg discharge energy into green light with 93% quantum efficiency,[2,4] illustrates the effectiveness of borate phosphor hosts. In this report we describe two new borates that stoichiometrically mimic the apatite compounds. The new materials $Sr_5(BO_3)_3F$ and $Sr_5(BO_3)_3Br$ have emerged from our study of the $SrO–B_2O_3–SrX_2$ (X = F, Cl, Br) phase systems.[5]

Here, we describe the structures of these compounds, each of which orders in separate space groups, and note their similarities. The previously reported material $Ca_5(BO_3)_3F$,[6] which differs structurally from the title compounds, has been compared to fluoroapatite, $Ca_5(PO_4)_3F$, illustrating the positional substitution of BO_3 triangles for PO_4 tetrahedra.[7] These comparisons will be extended here with a consideration of the new Sr compounds.

Experimental Section

Synthesis. A microcrystalline powder of $Sr_5(BO_3)_3Br$ was synthesized by using standard high-temperature solid-state techniques and high-purity reactants. $Sr_3(BO_3)_2$ was a laboratory-synthesized precursor formulated by heating a stoichiometric mixture of $Sr(NO_3)_2$ (AESAR, ACS grade) and anhydrous B_2O_3 (AESAR, 99.98%) at 900 K for 1 h, followed by additional heating at 1273 K for 24 h. A stoichiometric mixture of this reactant and anhydrous $SrBr_2$ (Alfa, 99%) was heated in a Pt crucible at 1073 K for 20 h. $Sr_5(BO_3)_3Br$ crystals were grown in a Pt crucible in air by cooling a melt of composition $SrO:B_2O_3:SrBr_2 = 57.0:12.8:30.2$ (mol %) at a rate of 8 K/h from 1200 to 1077 K and then rapidly cooling to room temperature. A clear prism of approximate dimensions 0.1 × 0.1 × 0.1 mm was physically separated from the matrix for single-crystal measurements described henceforward.

Because of the integrity of commercial SrF_2 at temperatures below 1200 K, we could not produce single-phase $Sr_5(BO_3)_3F$ by using the preceding synthesis temperature. However, reacting freshly prepared SrF_2 [$Sr(NO_3)_2$ heated under HF(g) at 800 K for 2–3 h] with $Sr_3(BO_3)_2$ at 1450 K in a Pt crucible afforded the title borate fluoride. Crystals were grown by melting the reactants at 1500 K and then cooling to 1000 K at a rate of 10 K/h. An alternate precipitation method was also found to be successful: $Sr(NO_3)_2$ and H_3BO_3 (AESAR, ACS grade) were dissolved in water with 10 mL of 8% (w/v) HF(aq), followed by gentle evaporation at ~350 K to dryness. Crystals were prepared by melting the resulting precipitate in a Pt crucible in air and cooling at 8 K/h from 1373 to 1223 K. An irregularly-shaped prism of approximate dimensions 0.15 × 0.10 × 0.20 mm from this crystal growth method was culled for X-ray study.

Crystallographic Study. The selected crystals were mounted on glass fibers and analyzed on a Rigaku AFC6R single-crystal X-ray diffractometer. The $Sr_5(BO_3)_3F$ unit cell parameters were accurately derived by a least-squares refinement of 19 automatically-centered reflections in the angular range $29 < 2\theta < 48°$. For the compound $Sr_5(BO_3)_3Br$, unit cell parameters were determined from 20 reflections within the limits $30 < 2\theta < 36°$. Intensity data for each borate halide were collected at room temperature by using the $\omega–2\theta$ scan technique with a rate of 16° (ω)/min and peak widths within $1.50 + 0.30 \tan \theta$. Three standard reflections demonstrated crystalline stability of $Sr_5(BO_3)_3F$ during the data collection, amounting to 1.6% maximum relative intensity deviation. A total of 1812 unique reflections ($F_o^2 > 3\sigma(F^2)$) were collected with $(\sin \theta_{max})/\lambda = 0.807$ Å^{-1} and the associated indices $0 \le h \le 14$, $0 \le k \le 19$, and $0 \le l \le 10$. Three standard peak orientations, measured every 200 reflections, indicated no intensity deterioration of $Sr_5(BO_3)_3Br$ throughout the collection, waiving the need for decay corrections. Of the 4764 measured reflections in the range $2 \le 2\theta \le 70°$ with corresponding indices $0 \le h \le 15$, $0 \le k \le 22$, and $-11 \le l \le 11$, a total of 2532 were observed [$F_o^2 > 3\sigma(F^2)$]. General crystallographic parameters are listed in Table I.

The atomic arrangements in the title compounds were determined by using programs contained in TEXSAN crystallographic software[8] with all calculations performed on a Digital μVAX II computer. The Sr$_5$-

---

(1) Soules, T.; Hoffman, M. In *Kirk-Othmer: Encyclopedia of Chemical Technology*, 3rd ed.; John Wiley & Sons: New York, 1981; Vol. 14, pp 527–545.

(2) Welker, T. *J. Lumin.* **1991**, *48/49*, 49–56.

(3) Chen, C.; Wu, Y.; Ru, L. *J. Cryst. Growth* **1990**, *99*, 790–798.

(4) Saubat, B.; Fouassier, C.; Hagenmuller, P. *Mater. Res. Bull.* **1981**, *16*, 193–198.

(5) Alekel, T.; Keszler, D. A. *Acta Crystallogr., Sect. C* **1992**, *48*, 1382–1386.

(6) Shirong, L.; Qingzhen, H.; Yifan, Z.; Aidong, J.; Chuangtian, C. *Acta Crystallogr., Sect. C* **1989**, *45*, 1861–1863.

(7) Fletcher J. G.; Glasser, F. P.; Howie, R. A. *Acta Crystallogr., Sect. C* **1991**, *47*, 12–14.

(8) TEXSAN. In *TEXRAY Structure Analysis Package*; Molecular Structure Corp.: The Woodlands, TX, 1985.

0020-1669/93/1332-0101$04.00/0

Table I. Crystallographic Data for $Sr_5(BO_3)_3F$ and $Sr_5(BO_3)_3Br$

chem formula	$Sr_5(BO_3)_3F$	$Sr_5(BO_3)_3Br$
fw	633.52	694.43
space group	*Pnma* (No. 62)	$C222_1$ (No. 20)
a, Å	7.220 (2)	10.002 (2)
b, Å	14.092 (2)	14.197 (1)
c, Å	9.810 (1)	7.458 (2)
V, Å^3	998.1 (5)	1059.0 (3)
Z	4	4
ρ_{calc}, g/cm^3	4.215	4.355
radiation	Mo Kα^a	Mo Kα^a
temp, K	298	298
linear abs coeff μ, cm^{-1}	258.0	280.2
transm factors	0.76–1.23	0.73–1.49
R, $R_w{}^b$	0.053, 0.057	0.057, 0.063

^{a} Graphite monochromated; $\lambda = 0.710\,69$ Å. ^{b} $R = \sum||F_o| - |F_c||/\sum|F_o|$; $R_w = [\sum w(|F_o|^2 - |F_c{}^2)^2/\sum w|F_o|^4]^{1/2}$.

$(BO_3)_3F$ data exhibit systematic absences $0kl$ ($k + l = 2n + 1$) and $hk0$ ($h = 2n + 1$) that are consistent with the two space groups $Pn2_1a$ and *Pnma*. Intensity statistics and the successful refinement support the assignment of the centric group.

The Sr atoms were located by using the direct methods program SHELXS[9a] and the anions and B atoms were positioned from successive analysis of difference electron density maps. Following refinement with isotropic displacement coefficients, the data were corrected for absorption with the program DIFABS[9b] and averaged ($R_{int} = 0.10$). The final refinement cycle with 825 observed F_o values, where $I > 3\sigma(I)$, included anisotropic displacement coefficients for the three heavy Sr atoms. The weighting scheme was based on counting statistics [$w = 1/\sigma^2(F_o)$] with $p = 0.05$. F_c was derived from predetermined neutral-atom scattering factors and corrected for anomalous scattering with calculated f' and f'' values from ref 10. The height of the largest peak in the final difference electron density map was 1.28% of the Sr2 atom.

For $Sr_5(BO_3)_3Br$, the noncentrosymmetric space group $C222_1$ is assigned unambiguously on the basis of the absences hkl ($h + k = 2n + 1$) and $00l$ ($l = 2n + 1$). Direct methods were employed to pinpoint the Sr atoms, while the remaining atoms were located from analysis of difference electron density maps. After the isotropic refinement of the best-fit $Sr_5(BO_3)_3Br$ enantiomer, the DIFABS empirical absorption correction was performed and ensued with a final least-squares refinement of $|F|$ with anisotropic displacement coefficients for every atom, barring B2. The final difference electron density map revealed a minimum peak of -4.22 Å^{-3} and a maximum peak of 6.51 e Å^{-3}, corresponding to 3.93% of the Sr3 atom peak intensity. The positional and thermal parameters for both structure solutions are outlined in Table II.

Results

$Sr_5(BO_3)_3F$. Figure 1 represents the unit cell of the compound. The structure is an intricate 3-dimensional framework of interconnecting Sr-centered polyhedra and BO_3 triangles. The framework can be simply described as two adjoined moieties that proliferate along the *b* axis: first, a double chain of Sr3-centered monocapped square antiprisms with B2 atoms situated among the special-position O atoms and, second, rows of F atoms encircled by Sr1/Sr2 polyhedra. The B1-centered borates assist in coupling the two moieties together.

The three Sr atom types possess distinctive coordination environments. The Sr1 atom assumes a distorted undecahedron coordinated by seven O atoms and one F atom. It shares O5··O6··F faces with two Sr2 atoms and two O1··O2··O6 faces with two Sr3 atoms. In addition, $Sr(1)O_7F$ shares edges with two B1 borates and corners with three B2 borates. The irregular 7-coordinated Sr2 site also contains an F atom in its periphery, along with six O atoms. Unlike the Sr1 site, $Sr(2)O_6F$ couples to itself by sharing O4··O6··F faces with two other Sr2 atoms. It also has an O3··O4 edge in common with an Sr3 atom and a common edge with the B2 borate, resting on a mirror plane. Additional borate connectivity is realized by three B1 groups that share corners with $Sr(2)O_7F$. The third Sr type is a distorted square antiprism that is monocapped by a weak O5 interaction. The $Sr(3)O_8$ + O polyhedra share mutual O1··O4··O6··O1 squares bases in the *ac* plane and triangular O1··O2··O3 faces in the *bc* plane, as viewed in Figure 2. A B1-centered borate shares the edge of O3 and the weakly-bound O5, while B2 atoms occupy trianglar sites along edges of the aforementioned condensed square bases.

Selected bond distances and angles for $Sr_5(BO_3)_3F$ are presented in Table III. For the Sr1 site, the Sr–O bond lengths range from 2.47 to 2.75 Å, bearing an average distance of 2.64 (3) Å, which closely matches the calculated crystal radius of 2.63 Å.[11] The average Sr2–O distance of 2.62 (2) Å, encompassing a spread of 2.49–2.81 Å, also correlates to the expected value. Possessing only O nearest neighbors, Sr3 atoms feature the widest variation of Sr–O distances (2.46–3.04 Å) and a greater average bond distance of 2.70 (3) Å.

The $Sr(3)O_9$ monocapped square antiprisms are moderately distorted with the Sr cation displaced from the center of the polyhedron along the *b* axis toward the capping O atom (see Figure 2). The O2/O3 base is not planar, with respective *b* axis distances of 0.98 and 0.64 Å from the medial cation. The capping O5 atom interacts with the Sr3 atom (3.04 Å) through this base, so all of these are general-position O atoms, accounting for the positional variability. However, the O1··O4··O6··O1 base is constrained to planarity by symmetry and situated 1.95 Å away from the Sr atom. The bases are not square, and their distortion can be described by an aspect ratio of the rectangular O–O side lengths projected onto the *ac* plane. For the O2/O3 base, the ratio characterizing its deviation from a square is 1.12. Additionally, both bases are not rectangular; the O2/O3 base exhibits an angle of 83.5° as a projected parallelogram. Because the other base contains three distinct O atoms, the O1/O4/O6 planar base assumes a quadrilaterial shape with an average aspect ratio of 1.34.

The Sr–F bond lengths of 2.40 and 2.42 Å for Sr1 and Sr2 fall short of the calculated distances 2.56 and 2.51 Å, respectively, from Shannon's fluoride radii,[12] indicating intimate bonding between the F atoms and both Sr types. Each F atom is surrounded by three bonding Sr atoms, but it does not reside in a triangular planar environment. Instead, the F atom is displaced from the center of the Sr1··Sr2··Sr2 triangle by 0.92 Å, forming two Sr1–F–Sr2 bond angles of 109.9 (4)° and one Sr2–F–Sr2 angle of 98.0 (4)°; the site symmetry is C_s.

The two borate types in $Sr_5(BO_3)_3F$ assume regular orthoborate geometry but deviate from the ideal trigonal planar configuration. The $B(1)O_3$ group exhibits a slightly compressed B1–O2 bond length of 1.36 Å with an average distance of 1.39 (3) Å. The B2-centered triangle features C_{2v} point symmetry with an elongated B2–O1 bond length of 1.41 Å and an average distance of 1.37 (4) Å. Both borate types maintain O–B–O bond angles within 3° of the 3-fold symmetrical 120° angle.

$Sr_5(BO_3)_3Br$. The unit cell for the compound is depicted in Figure 3. It is isostructural with the $Sr_5(BO_3)_3Cl$ analogue, which we have previously described.[5] At a casual glance, it appears to be identical to the fluoride title compound, but upon continued examination, one recognizes a sizable shift in the halide position between the two. Six Sr atoms coordinate to each Br atom, constituting a distorted octahedron with opposite triangular Sr faces canted toward one another in the *b* direction; linked together by common faces, the octahedra form chains that extend along the *c* axis.

One of the Sr types that coordinates to the Br atom occupies a distorted tricapped trigonal prism [$Sr(1)O_7Br_2$]; it shares Br

---

(9) (a) Sheldrick, G. SHELXS86. In *Crystallographic Computing 3*; Sheldrick, G., Krüger, C., Goddard, R., Eds.; Oxford University Press: New York, 1985; pp 175–189. (b) Walker, N.; Stuart, D. *Acta Crystallogr., Sect. A* **1983**, *39*, 158–166.

(10) *International Tables for X-ray Crystallography*; Kynoch Press: Birmingham, England, 1974; Vol. IV.

(11) Shannon, R.; Prewitt, C. *Acta Crystallogr., Sect. B* **1968**, *25*, 925–946.

(12) Shannon, R. *Acta Crystallogr., Sect. A* **1976**, *32*, 751–767.

Table II. Positional Parameters for $Sr_5(BO_3)_3F$ and $Sr_5(BO_3)_3Br$

	$Sr_5(BO_3)_3F$				$Sr_5(BO_3)_3Br$[a]			
	x	y	z	B_{eq},[b] Å^2	x	y	z	B_{eq}, Å^2
Sr1	0.2887 (3)	$^1/_4$	0.4814 (2)	0.33 (6)	0.2404 (3)	0	0	1.5 (1)
Sr2	0.2490 (2)	0.3801 (1)	0.1260 (1)	0.54 (4)	0.8665 (2)	0.1289 (1)	0.0645 (3)	1.3 (1)
Sr3	0.0286 (2)	0.3880 (1)	0.7470 (2)	0.36 (4)	$^1/_2$	0.1355 (2)	$^1/_4$	1.2 (1)
Sr4					$^1/_2$	0.8620 (2)	$^1/_4$	1.4 (1)
F/Br	0.135 (2)	$^1/_4$	0.265 (1)	0.8 (2)	0	0.9429 (4)	$^1/_4$	2.4 (2)
O1	0.283 (2)	$^1/_4$	0.748 (1)	0.3 (2)	0.492 (2)	0	0	1.3 (7)
O2	0.774 (2)	0.4301 (7)	0.930 (1)	0.8 (2)	0.330 (1)	0.192 (1)	0.988 (2)	1.4 (6)
O3	0.281 (1)	0.4543 (7)	0.8956 (8)	0.6 (1)	0.644 (1)	0.199 (1)	0.020 (2)	1.5 (6)
O4	0.119 (2)	$^1/_4$	0.955 (2)	0.7 (2)	0.305 (1)	0.997 (1)	0.659 (2)	1.9 (6)
O5	0.910 (2)	0.0902 (9)	0.153 (1)	1.0 (2)	0.166 (1)	0.146 (1)	0.112 (2)	1.5 (6)
O6	0.445 (2)	$^1/_4$	0.963 (2)	0.9 (3)				
B1	0.799 (2)	0.040 (1)	0.061 (1)	0.4 (2)	0.199 (2)	0.212 (2)	0.028 (3)	1.0 (1)
B2	0.286 (3)	$^1/_4$	0.891 (2)	0.1 (3)	0.629 (3)	0	0	0.8 (5)

[a] To convert the $C222_1$ cell to the $Sr_5(BO_3)_3F$ *Pnma* cell, use the following translational transformation:

$$\begin{bmatrix} 0 & 0 & 1 \\ 0 & -1 & 0 \\ 1 & 0 & 0 \end{bmatrix} + \begin{bmatrix} 0.2886 \\ 0.2500 \\ 0.4710 \end{bmatrix}$$

[b] $B_{eq} = (8\pi^2/3)\sum_i\sum_j U_{ij}a_i^*a_j^*\mathbf{a}_i\cdot\mathbf{a}_j$.

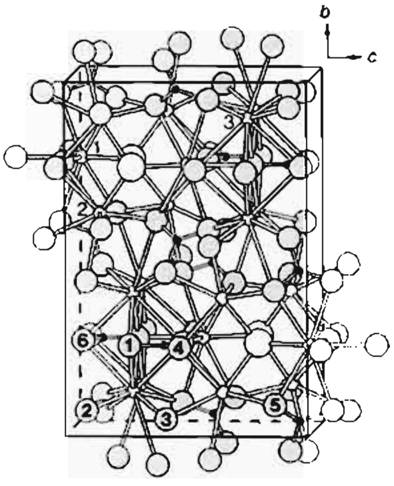

Figure 1. Schematic unit-cell drawing of $Sr_5(BO_3)_3F$. The small open circles represent Sr atoms, the large shaded circles represent O atoms, the small black circles represent B atoms, and the large open circles represent F atoms (atomic legend used in subsequent figures, unless noted). The Sr and O atoms are numerically labeled.

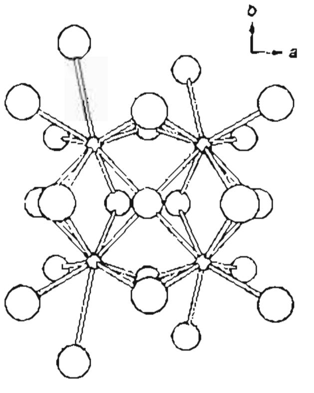

Figure 2. Sr3-centered distorted monocapped square antiprisms in $Sr_5(BO_3)_3F$, illustrating the three- and four-point face-sharing of the polyhedra. The monocapping interaction is 3.04 Å.

corners with adjacent Sr1 polyhedra along the 2_1 screw axis to form a zigzag chain. The nonacoordinate Sr1 centers share faces with Sr2-centered polyhedra and with the $Sr(3)O_8/Sr(4)O_8$ distorted square antiprisms. Four irregular $Sr(2)O_6Br_2$ undecahedra also surround each Br atom, connecting to one another along the *c* axis via common Br--Br--O4--O4 and Br--O5--O5 faces. The Sr2 polyhedra are linked together by $B(1)O_3$ borate groups in the *a* and *b* directions, as well.

Table III. Selected Bond Distances (Å) and Angles (deg) for $Sr_5(BO_3)_3F$

Sr1–F	2.40 (1)	F–Sr1–O2	105.6 (2)
Sr1–O1	2.61 (1)	O1–Sr1–O2	71.1 (2)
Sr1–O2	2.69 (1)	O1–Sr1–O4	76.1 (5)
Sr1–O2	2.69 (1)	O2–Sr1–O4	87.8 (3)
Sr1–O4	2.47 (1)	O4–Sr1–O5	79.3 (3)
Sr1–O5	2.75 (1)	F–Sr1–O5	73.9 (3)
Sr1–O5	2.75 (1)	O2–Sr1–O5	52.8 (3)
Sr1–O6	2.54 (2)	O2–Sr1–O6	83.9 (3)
Sr2–F	2.43 (1)	F–Sr2–O4	73.4 (4)
Sr2–O2	2.74 (1)	O2–Sr2–O3	54.2 (3)
Sr2–O3	2.50 (1)	O2–Sr2–O5	92.2 (3)
Sr2–O4	2.49 (1)	O3–Sr2–O4	75.5 (3)
Sr2–O5	2.49 (1)	O3–Sr2–O6	83.4 (3)
Sr2–O5	2.50 (1)	O4–Sr2–O5	80.7 (4)
Sr2–O6	2.81 (1)	O4–Sr2–O6	50.9 (4)
Sr3–O1	2.68 (1)	O1–Sr3–O1	85.7 (1)
Sr3–O1	2.63 (1)	O1–Sr3–O4	49.7 (4)
Sr3–O2	2.63 (1)	O2–Sr3–O3	91.5 (3)
Sr3–O2	2.55 (1)	O2–Sr3–O5	70.8 (3)
Sr3–O3	2.51 (1)	O3–Sr3–O5	86.1 (3)
Sr3–O3	2.46 (1)	O3–Sr3–O6	72.4 (3)
Sr3–O4	2.89 (1)	O4–Sr3–O6	95.6 (2)
Sr3--O5	3.04 (1)	O4–Sr3–O5	111.7 (3)
Sr3–O6	2.90 (1)	O2–Sr3–O6	79.4 (4)
B1–O2	1.36 (2)	O2–B1–O3	120 (1)
B1–O3	1.40 (2)	O2–B1–O5	122 (1)
B1–O5	1.41 (2)	O3–B1–O5	118 (1)
B2–O1	1.41 (2)	O1–B2–O4	117 (2)
B2–O4	1.35 (2)	O1–B2–O6	122 (2)
B2–O6	1.35 (3)	O4–B2–O6	121 (2)

The association between the Sr3 and Sr4 square antiprisms is similar to those arranged in $Sr_5(BO_3)_3F$, minus the additional monocapping O atom. Besides sharing triangular faces in the *ab* direction, the antiprisms incorporate B2 atoms that are confined in the *ac* plane square bases. Both $Sr(3)O_8$ and $Sr(4)O_8$ polyhedra share O2/O3 corners with $B(1)O_3$ triangles that bridge to Sr2 undecahedra. The square antiprisms also adjoin with $Sr(2)O_6Br_2$ polyhedra via O3--O4--O4 faces.

Selected bond distances and angles are listed for $Sr_5(BO_3)_3Br$ in Table IV. Two Br atoms bond to Sr1 at a distance of 3.149 (2) Å, which exceeds the calculated length of 3.08 Å from crystal radii. The average Sr1–O bond length of 2.66 (3) Å compares to the 2.68-Å average span of the nonacoordinate SrO_9 site in $Sr_6YAl(BO_3)_6$[13] and approximates the calculated distance of 2.63 Å. The broad range of Sr2–O bond lengths (2.43–3.04 Å) and the dissimilar Sr2–Br distances (3.266 and 2.884 Å) define the irregular shape of the $Sr(2)O_6Br_2$ undecahedron.

---

(13) Schaffers, K. I.; Thompson, P. D.; Alekel, T.; Cox, J. R.; Keszler D. A. *Chem. Mater.*, submitted for publication.

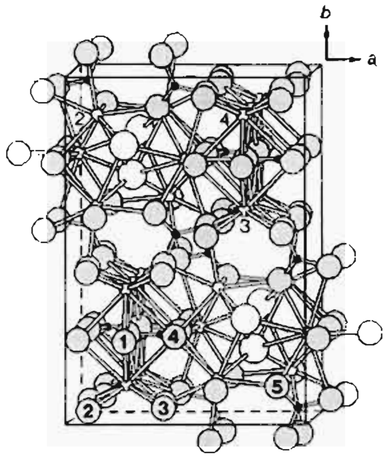

Figure 3. Schematic unit-cell drawing of $Sr_5(BO_3)_3Br$. The large open circles represent Br atoms; the Sr and O atoms are numericlly labeled.

Table IV. Selected Bond Distances (Å) and Angles (deg) for $Sr_5(BO_3)_3Br$

Sr1–Br	3.149 (2)	Br–Sr1–O4	67.6 (3)
Sr1–Br	3.149 (2)	Br–Sr1–O5	68.8 (3)
Sr1–O1	2.51 (2)	O1–Sr1–O2	71.8 (2)
Sr1–O2	2.87 (1)	O2–Sr1–O4	84.8 (5)
Sr1–O2	2.87 (1)	O2–Sr1–O5	52.8 (4)
Sr1–O4	2.63 (1)	O4–Sr1–O4	151.3 (6)
Sr1–O4	2.63 (1)	O1–Sr1–O4	75.6 (3)
Sr1–O5	2.56 (1)	O4–Sr1–O5	78.0 (5)
Sr1–O5	2.56 (1)	O5–Sr1–O5	121.3 (6)
Sr2–Br	3.266 (5)	Br–Sr2–O4	73.4 (4)
Sr2–Br	2.884 (3)	Br–Sr2–Br	82.5 (1)
Sr2–O2	2.60 (1)	O2–Sr2–O3	56.9 (3)
Sr2–O3	2.46 (1)	O3–Sr2–O4	70.5 (4)
Sr2–O4	3.04 (2)	Br–Sr2–O4	88.1 (3)
Sr2–O4	2.58 (2)	O4–Sr2–O4	49.1 (6)
Sr2–O5	2.53 (1)	Br–Sr2–O4	67.0 (3)
Sr2–O5	2.43 (1)	O4–Sr2–O5	80.9 (5)
Sr3–O1	2.680 (2)	O1–Sr3–O1	88.3 (1)
Sr3–O1	2.680 (2)	O1–Sr3–O4	70.3 (4)
Sr3–O2	2.71 (1)	O1–Sr3–O2	72.0 (4)
Sr3–O2	2.71 (1)	O2–Sr3–O4	86.3 (4)
Sr3–O3	2.42 (2)	O1–Sr3–O3	78.3 (4)
Sr3–O3	2.42 (2)	O2–Sr3–O3	91.2 (4)
Sr3–O4	2.79 (2)	O3–Sr3–O4	70.5 (4)
Sr3–O4	2.79 (2)	O4–Sr3–O4	95.0 (6)
Sr4–O1	2.706 (2)	O1–Sr4–O1	87.1 (1)
Sr4–O1	2.706 (2)	O1–Sr4–O4	68.7 (5)
Sr4–O2	2.57 (2)	O1–Sr4–O2	73.5 (4)
Sr4–O2	2.57 (2)	O2–Sr4–O4	85.5 (4)
Sr4–O3	2.63 (1)	O1–Sr4–O3	74.3 (4)
Sr4–O3	2.63 (1)	O2–Sr4–O3	94.1 (4)
Sr4–O4	2.87 (2)	O3–Sr4–O4	71.1 (5)
Sr4–O4	2.87 (2)	O4–Sr4–O4	91.8 (6)
B1–O2	1.38 (3)	O2–B1–O3	121 (2)
B1–O3	1.42 (3)	O2–B1–O5	120 (2)
B1–O5	1.41 (3)	O3–B1–O5	119 (2)
B2–O1	1.38 (4)	O1–B2–O4	119 (1)
B2–O4	1.35 (2)	O1–B2–O4	119 (1)
B2–O4	1.35 (2)	O4–B2–O4	122 (3)

In its square antiprism, the Sr3 atom is displaced from the O1/O4 plane by 1.92 Å and from the O2/O3 plane by 0.85 Å. The respective distances for the Sr4 atomic position are 1.96 and 0.85 Å. For the rectangular O1/O4 base defining the Sr3 site (and the analogous Sr4 site parameters following parenthetically), the ratio characterizing its deviation from equal side lengths (projected onto the *ac* plane) is 1.32 (1.32), while the O2/O3 base aspect ratio is 1.17 (1.19). Both projected bases are parallelograms with internal angles of 83.5 (83.5) and 82.8° (89.0°) for the respective O1/O4 and O2/O3 bases. A regular square antiprism maintains a twist angle between the bases of 45°, but in the title bromide, the twist angle between the bases, as approximated by the *b*-axis-projected O3–Sr3–O4 (O1–Sr4–O2) angle, is 32° (41°).

The two B atoms constitute slightly distorted orthoborates [$B(1)O_3$ and $B(2)O_3$ exhibit C_s and C_{2v} symmetry, respectively] with collective O–B–O angles that range between 119 and 122° and that average 120 (4)°. The B1-centered triangle is larger than the symmetrical B2 borate; the average B1–O distance is 1.41 (3) Å, while the average B2–O length is 1.37 (3) Å.

Discussion

Symmetry Relationships. The atomic positions in the $Sr_5(BO_3)_3Br$ unit cell can be converted to closely match those of the centric title fluoride for direct comparison. With the Sr1 atoms in each structure assigned to be spatially equivalent, the cell transformation matrix and translational vector presented in Table II generate a cell analogous to $Sr_5(BO_3)_3F$. The following discussion refers to the transformation of the title bromide atomic locations to the centric reference framework $Sr_5(BO_3)_3F$ (*C*222$_1$ ⇒ *Pnma*).

The distinction between the two structures is best illustrated by the position of the halides in each matrix. The Br atom is displaced from the corresponding F atom in $Sr_5(BO_3)_3F$ by roughly 10, 5, and 0.5% of a unit cell dimension in the respective *a*, *b*, and *c* directions. The resulting changes in symmetry of this shift are 2-fold. First, the face-centering element of the *C*222$_1$ lattice disappears in the title fluoride *Pnma* arrangement; the zigzag chains of Br sites observed along the *c* screw axis, a consequence of the centering origin ($^1/_2$, $^1/_2$, 0), contrasts with the in-line F atoms similarly viewed in $Sr_5(BO_3)_3F$. Second, a center of inversion in the title fluoride is not present in $Sr_5(BO_3)_3Br$. This is also visualized by the different halide positions between both structures. Because the F atom resides on a *b* axis mirror plane in *Pnma*, the four collective F atoms in the unit cell are centrosymmetrically related, unlike the zigzag Br atom arrangement in *C*222$_1$.

The other types of atomic shifts within the unit cells are henceforth described. The Sr3 cations exhibit a nominal difference in position between the two structures, but the Sr2 atoms exhibit a large spatial dissimilarity in the *ac* plane. Every O type notably differs in location between the two compounds, repositioned by 1–100 *σ*. The B2 atoms that fit within the shared faces of the square antiprisms show little deviation, but the bridging B1-centered borates show a small displacement in the *a* direction, nearly orthogonal to the triangular plane, causing a tilt of the BO_3 groups in the fluoride relative to the bromide that conforms to inversion symmetry of the *Pnma* cell.

Although many of the corresponding atomic positions between the two title structures are very similar, the aforementioned deviations modify several site geometries. As stated previously, the most dramatic observed difference involves the Sr sites that interact with F/Br atoms. Rather than possessing two halide atoms in their coordination sphere, as Sr1 and Sr2 in $Sr_5(BO_3)_3Br$, the Sr1 and Sr2 atoms in $Sr_5(BO_3)_3F$ bond with only one F atom per site. The F atom next-nearest to the Sr1 and Sr2 atoms is positioned 3.48 and 3.50 Å away, respectively—far too long to form a second Sr–F interaction per site.

Bond Valence Calculations. We were curious about the Sr coordination environments, especially the degree of bonding at the Sr3 site in the $Sr_5(BO_3)_3F$ structure. Brown's empirical bond valence method[14] was implemented to determine the extent of interaction between Sr and O or F atoms. Because no parameters are available for bonds between Sr and Br, we were limited to strictly Sr–O calculations for $Sr_5(BO_3)_3Br$; nevertheless, we were able to analyze each Sr type in the fluoride structure.

Each of the Sr atom sites in $Sr_5(BO_3)_3F$ experiences distinctive bonding geometries. The eight anions of the $Sr(1)O_7F$ site decisively bond to the Sr atom, yielding a total valence sum of

---

(14) Brown, I. D. In *Structure and Bonding in Crystals*; Academic Press: New York, 1981; Vol. II, Chapter 14.

1.97, which closely matches formal alkaline-earth-metal divalency. In contrast, even though every nearest neighbor anion significantly interacts with the Sr2 atom, the lower number of surrounding anions at the $Sr(2)O_6F$ site reduces the Sr atom, as evidenced by the calculated total bond valence of 1.85. The distorted square antiprismatic Sr3 site achieves a completed calculated valency of 2.02. However, a 3.04-Å Sr–O distance was initially questioned as an actual bond, but upon evaluation of the calculated Sr3 bond valency, we considered the 4.3% contribution to be significant.

Of the two distorted square antiprismatic sites in the $Sr_5(BO_3)_3Br$ structure, the Sr3 atom is suggested by the valence determination to have a completed bonding environment, possessing a calculated valency of 1.99. However, the structural dissimilarity of the $Sr(4)O_8$ antiprism from the Sr3 site affects the calculated valency of 1.67. No other anions reside nearby to make up the covalent deficiency, unlike the mirror plane symmetric square antiprisms in the $Sr_5(BO_3)_3F$ structure that have a long bond to a ninth O atom.

Structure Comparisons. $Sr_5(BO_3)_3Cl$[5] and $Sr_5(BO_3)_3Br$ have no alkaline-earth-metal stoichiometric homologues for comparison, but $Sr_5(BO_3)_3F$ can be compared to two other fluorides that have been previously described: $Ca_5(BO_3)_3F$ and $Mg_5(BO_3)_3F$.[6,15] They arrange in separate space groups, *Cm* and *Pna*2₁, respectively. Even though the noncentrosymmetric orthorhombic space group $Pna2_1$ of the magnesium borate fluoride is simply a subgroup of the title fluoride (*Pnma*), the atomic arrangement notably differs between the two: chains of Mg-centered, edge-sharing octahedra, interconnected by BO_3 triangles, define the framework. The Ca atoms in $Ca_5(BO_3)_3F$ also occupy distorted octahedral sites that are linked by corner-sharing BO_3 groups. The title fluoride requires larger sites of higher coordination to accommodate the Sr atom. The various Sr polyhedra not only extensively share faces and edges with each other, but the two edge- and corner-sharing borate groups also contribute to the high degree of connectivity in $Sr_5(BO_3)_3F$.

The F atom environment of this series also demonstrates the variation of the three compounds. The cationic grouping about the F atom in the $Mg_5(BO_3)_3F$ structure is triangular with each Mg atom residing in a unique octahedral site. Thus, three of the five Mg octahedra types include one F atom. Similarly, the F atom in $Sr_5(BO_3)_3F$ is 3-fold coordinated, but it is bonded to only two Sr atom types, both with one F atom per polyhedron. In contrast, the F atom in $Ca_5(BO_3)_3F$ is situated in a slightly distorted tetrahedral site created by two Ca types. The F atom is shared between two octahedral sites, $Ca(2)O_4F_2$ and $Ca(3)O_5F$. From this homologous series [$A_5(BO_3)_3F$; A = Mg, Ca, Sr], it is evident that the cation requirements of size and bonding coordination ultimately determine the atomic arrangement of these compounds.

The polyatomic anion substitution of BO_3 in $Ca_5(BO_3)_3F$ for the phosphate in fluoroapatite, $Ca_5(PO_4)_3F$, has previously been described,[7] but the parallel strontium haloapatite stoichiometric analogues [$Sr_5(PO_4)_3F$ or $Sr_5(PO_4)_3Br$] of $Sr_5(BO_3)_3F$ and $Sr_5(BO_3)_3Br$ have not been structurally reported. Even so, because of the importance of the phosphate as laser hosts[16] and phosphors, we compare here the alkaline-earth-metal environments of $Sr_5(PO_4)_3Cl$[17] and $Ca_5(PO_4)_3F$[18] to those of the title structures (see Figure 4). The two phosphate structures primarily differ in the positions of the halide anions. Each apatite has two cations on special positions with C_3 and C_s site symmetries; the former site consists of nine O atoms around the metal center, but the latter is either $Sr(2)O_6Cl_2$ or $Ca(2)O_6F$, depending on the position of the halide in the structure. Subsequently, the Cl^- anion is octahedrally coordinated by Sr atoms, while the F^- anion is trigonally surrounded by three Ca nearest neighbors. Like the Sr2-centered polyhedra in $Sr_5(PO_4)_3Cl$ that interconnect by sharing mutual Cl edges, one $Sr(1)O_7Br_2$ and two $Sr(2)O_6Br_2$ polyhedra in $Sr_5(BO_3)_3Br$ trilaterally share a Br···Br edge. As a result, the Br anion is also bonded to six cations. The distorted pentagonal bipyramid Ca2 sites in $Ca_5(PO_4)_3F$ are joined through a common F corner. Likewise, in $Sr_5(BO_3)_3F$, one $Sr(1)O_7F$ and two $Sr(2)O_6F$ polyhedra triangularly coordinate a single F atom.

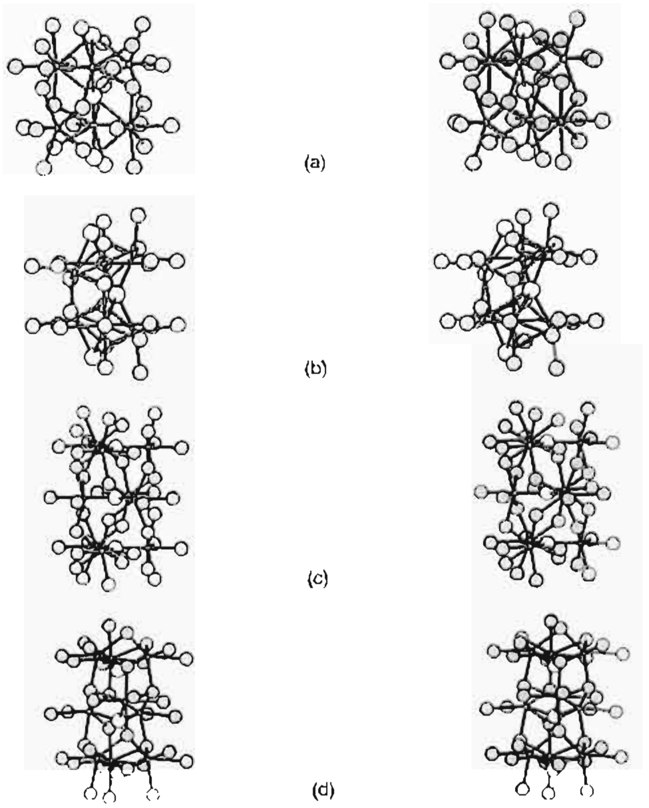

Figure 4. Stereoviews illustrating the connectivity of the alkaline-earth-metal centered polyhedra that coordinate to the columns of halides within the following labeled structures: (a) $Sr_5(PO_4)_3Cl$; (b) $Sr_5(BO_3)_3Br$; (c) $Ca_5(PO_4)_3F$; (d) $Sr_5(BO_3)_3F$. The small open circles portray the alkaline-earth metal, and the large open circles represent the halide. The *c* axis is vertical in the page except for the case of (d), where the *a* axis is vertical.

Acknowledgment. This research was supported by the U.S. National Science Foundation, Solid-State Chemistry Program (Grant DMR-8814432). Acknowledgment is made to the donors of the Petroleum Research Fund, administered by the American Chemical Society, for partial support of this research. D.A.K. thanks the Alfred P. Sloan Research Foundation for a fellowship.

Supplementary Material Available: Tables listing complete crystallographic and data collection information and anisotropic thermal parameters and schematic stereoviews of the unit cells (4 pages). Ordering information is given on any current masthead page.

---

(15) Brovkin, A.; Nikishova, L. *Sov. Phys. Crystallogr.* **1975**, *20*, 252–254.
(16) Huber, G.; Lutz, F. *J. Cryst. Growth* **1981**, *52*, 646–649.
(17) Sudarsanan, K.; Young, R. A. *Acta Crystallogr., Sect. B* **1974**, *30*, 1381–1386.
(18) Sudarsanan, K.; Mackie, P. E.; Young, R. A. *Mater. Res. Bull.* **1972**, *7*, 1331–1338.